EUKARYOTIC CELL, Nov. 2007, p. 2018–2028 Vol. 6, No. 11
1535-9778/07/$08.00+0 doi:10.1128/EC.00210-07

Cryptosporidium parvum Long-Chain Fatty Acid Elongase▽†

Jason M. Fritzler,[1] Jason J. Millership,[1]‡ and Guan Zhu[1,2]*

Department of Veterinary Pathobiology, College of Veterinary Medicine & Biomedical Sciences,[1] and Faculty of Genetics Program,[2] Texas A&M University, College Station, Texas 77843-4467

Received 18 June 2007/Accepted 28 August 2007

We report the presence of a new fatty acyl coenzyme A (acyl-CoA) elongation system in *Cryptosporidium* and the functional characterization of the key enzyme, a single long-chain fatty acid elongase (LCE), in this parasite. This enzyme contains conserved motifs and predicted transmembrane domains characteristic to the elongase family and is placed within the ELO6 family specific for saturated substrates. Cp*LCE1* gene transcripts are present at all life cycle stages, but the levels are highest in free sporozoites and in stages at 36 h and 60 h postinfection that typically contain free merozoites. Immunostaining revealed localization to the outer surface of sporozoites and to the parasitophorous vacuolar membrane. Recombinant CpLCE1 displayed allosteric kinetics towards malonyl-CoA and palmitoyl-CoA and Michaelis-Menten kinetics towards NADPH. Myristoyl-CoA ($C_{14:0}$) and palmitoyl-CoA ($C_{16:0}$) display the highest activity when used as substrates, and only one round of elongation occurs. CpLCE1 is fairly resistant to cerulenin, an inhibitor for both type I and II fatty acid synthases (i.e., maximum inhibitions of 20.5% and 32.7% were observed when $C_{16:0}$ and $C_{14:0}$ were used as substrates, respectively). These observations ultimately validate the function of CpLCE1.

As one of the vital compounds for all organisms, fatty acids of 14 to 18 carbons in length comprise the bulk of cellular fatty acids that serve structural and biological functions, and they are usually the major products of de novo synthesis in most cells. These long-chain fatty acids play important roles in many biological functions such as energy metabolism and membrane structure. There are several metabolic pathways that produce long-chain fatty acids, most notably the type I and type II fatty acid synthases (FASs). The type I enzymes of mammals and fungi are typically cytosolic and composed of multiple enzymes arranged into domains of one or two large polypeptides (31). In contrast, the enzymes of the type II FASs are all located on separate domains and are found in prokaryotes or in eukaryotic organelles of prokaryotic origin (33).

Relatively common among eukaryotic organisms are the fatty acid elongase-based systems. These elongase-based systems directly elongate a fatty acyl chain esterfied with CoA (fatty acyl-CoA), which is in contrast to the type I and type II FAS systems, which elongate a fatty acyl chain attached to an acyl carrier protein. The elongase system is comprised of at least four enzymes that are responsible for adding two carbon units to the fatty acyl carboxyl end. The chemistry of this pathway is similar to that used by type I and type II FASs. Fatty acyl elongation begins with the condensation of malonyl-CoA with a fatty acyl-CoA catalyzed by the condensing enzyme LCE (β-ketoacyl-CoA synthase) (Fig. 1, step 1). The resulting β-ketoacyl-CoA is then two carbons longer and is subsequently reduced to β-hydroxyacyl-CoA in an NAD(P)H-dependent reaction by β-ketoacyl-CoA reductase (Fig. 1, step 2). Dehydration occurs through the action of β-hydroxyacyl-CoA dehydratase to yield enoyl-CoA (Fig. 1, step 3), which is further reduced by enoyl-CoA reductase in an NAD(P)H-dependent manner (Fig. 1, step 4) to yield the elongated fatty acyl-CoA. Whether or not the elongated product is released for use elsewhere in the cell or is retained to undergo another round of elongation depends largely on the specific needs of the organism.

Although purification and biochemical characterization of these four enzymes are difficult due to their membrane-bound nature, it appears that the condensing enzyme is the rate-limiting enzyme of the elongase system, and it is commonly referred to as "elongase" (4, 8, 24). Thus, it is responsible for the fatty acid substrate specificity regarding chain length and pattern of double bonds, whereas the other three components of the elongase system display little or no particular substrate specificity (8). Comparative protein sequence analysis has classified the condensing enzymes into two distinct groups: the KCS/fatty acid elongation group, present mainly in plants, and the elongase (ELO) group, present in protozoa, mammals, and fungi (16). It is not uncommon for a cell or organism to contain multiple condensing enzymes that share the same reductase-dehydratase-reductase enzymes. Furthermore, each system within a cell or organism may exhibit a broad range of substrate specificities (sometimes overlapping) for fatty acid chain length as well as saturated or unsaturated fatty acids (16). For example, *Saccharomyces cerevisiae* contains three elongases termed ELO1, ELO2, and ELO3, in which ELO1 has a preference for elongating C_{12} to C_{16} fatty acids, whereas ELO2 and ELO3 elongate C_{16} saturated and monounsaturated fatty acids to C_{24} and C_{26}, respectively (27). This study aims to characterize the sole long-chain elongase from *Cryptosporidium parvum* (CpLCE1) and is the first such study among the apicomplexan parasitic protozoa.

* Corresponding author. Mailing address: Department of Veterinary Pathobiology, College of Veterinary Medicine & Biomedical Sciences, Texas A&M University, 4467 TAMU, College Station, TX 77843-4467. Phone: (979) 845-6981. Fax: (979) 845-9972. E-mail: gzhu@cvm.tamu.edu.

† Supplemental material for this article may be found at http://ec.asm.org/.

‡ Present address: Fort Dodge Animal Health, 800 5th Street, N.W., Fort Dodge, IA 50501.

▽ Published ahead of print on 7 September 2007.

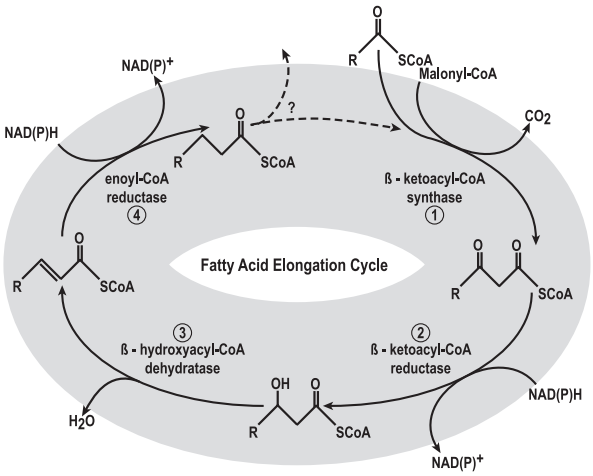

FIG. 1. The fatty acid elongation system. The diagram displays the four enzymes and fatty acyl-CoA intermediates involved in the two-carbon elongation of fatty acyl-CoAs. The first step is a condensation reaction catalyzed by the "elongase" enzyme (CpLCE1). This is the enzyme that determines chain length and degree of unsaturation of the substrate, and it is the rate-limiting step of the system. The product of the condensation reaction then undergoes reduction by a β-ketoacyl-CoA reductase (step 2), dehydration by β-hydroxyacyl-CoA dehydratase (step 3), and a final reduction by enoyl-CoA reductase (step 4). Whether or not the elongated product is utilized elsewhere in the cell or organism or undergoes an additional round(s) of elongation depends largely on the needs of the specific cell/organism at that time.

MATERIALS AND METHODS

Identification of CpLCE1 and phylogenetic reconstructions. The Cp*LCE1* gene was originally identified from a *C. parvum* genome contig by homology searches and was then cloned and sequenced to confirm its identity (GenBank accession No. AAO34582). It was later annotated in the genome sequencing projects as a "7 pass integral membrane protein with FLHWFHH motif shared with fatty-acyl elongase" for *C. parvum* (XP_627348) and as "fatty-acyl elongase" for *Cryptosporidium hominis* (XP_666343).

To determine the evolutionary relationship of CpLCE1 to elongases from other organisms, we performed maximum-likelihood (ML)-based phylogenetic analyses. The CpLCE1 amino acid sequence was used as a query to search protein databases, including all nonredundant GenBank CDS translations, RefSeq Proteins, PDB, SwissProt, PIR, and PRF at the National Center for Biotechnology Information (NCBI), using the PSI-BLAST program (http://www.ncbi.nlm.nih.gov/BLAST) (2). Elongase sequences from other apicomplexans were also obtained from http://PlasmoDB.org (*Plasmodium*) and http://ToxoDB.org (*Toxoplasma gondii*). Four iterative BLAST searches were performed, and only sequences with *E* values of better than 1×10^4 were selected for phylogenetic analysis.

Multiple-sequence alignments were performed on 75 sequences using the ClustalW algorithm housed in the MacVector v9.5.2 program (MacVector, Inc.), and apparent mistakes in alignment were corrected upon visual inspection. A data set containing 91 unambiguously aligned amino acid positions was used in subsequent analysis. The MrBayes v3.1.2 program (http://mrbayes.csit.fsu.edu/) was used to reconstruct trees using a Bayesian inference method (12). The program was allowed to "jump" among all available amino acid substitution models and to consider among-site rate heterogeneity using a fraction of invariance (*Inv*) plus a four-rate Γ-distribution model during Markov chain Monte Carlo analysis. A total of 5×10^6 generations of searches were performed with two independent runs, each containing four chains simultaneously running. The current trees were saved every 1,000 generations. Posterior probability (PP) values at tree nodes were obtained by calculating consensus trees from the last 3,000 Bayesian inference trees that were obtained after the runs converged. In addition, ML analysis was also performed using the PROML program included in the PHYLIP package (http://evolution.gs.washington.edu/phylip.html). The Jones-Taylor-Thornton model (14), with the consideration of *Inv* and four-rate Γ that were estimated using the TREE-PUZZLE v.5.2 program (http://www.tree-puzzle.de).

Transcript analysis for CpLCE1 at various developmental stages. Freshly isolated *C. parvum* oocysts (Iowa strain) purified by Percoll gradient centrifugation and stored in water at 4°C (3) were used to analyze the relative transcript levels for the Cp*LCE1* gene. Oocysts were excysted in phosphate-buffered saline (PBS) containing 0.1% trypsin and 0.5% taurodeoxycholic acid for 90 min at 37°C to release free sporozoites, which were further purified using a Percoll gradient centrifugation method (29). Intracellular stages of *C. parvum* were obtained by infecting human HCT-8 cells with oocysts for various times (6 to 72 h). Total RNA was isolated from oocysts, free sporozoites, and intracellular stages using an RNeasy kit (QIAGEN) following the manufacturer's recommended protocol for animal cells. The only addition to RNA isolation using this method was that oocysts were suspended in the recommended lysis buffer and underwent 10 freeze-thaw cycles (liquid nitrogen and 37°C) to disrupt the oocyst wall prior to RNA isolation.

A SYBR green-based real time quantitative reverse transcription-PCR (qRT-PCR) method was used to determine the transcript levels of Cp*LCE1* at the various developmental stages. The primer pair CpLCE1-F07 (5′ TCA CTT TAT CAG AAC CAA CGG TG 3′) and CpLCE1-R07 (5′ GGC AGT TAC CCA TTC AGC AAG 3′) was used to amplify Cp*LCE1* transcripts. To amplify *C. parvum* 18S rRNA as a control for normalization, we used the previously reported primers 995F (5′ TAG AGA TTG GAG GTT GTT CCT 3′) and 1206R (5′ CTC CAC CAA CTA AGA ACG GCC 3′) (1). The relative level of Cp*LCE1* transcripts was expressed relative to that of 18S rRNA, and values are reported based on at least three replicates as previously described (5, 28).

Production of antibodies. A short peptide corresponding to a unique internal sequence of CpLCE1 (^{76}FGPKIMEKRKPFKLEKPLKYW) (Fig. 2) was synthesized by the Peptide Core Facility at the Department of Veterinary Pathobiology, Texas A&M University. This short peptide is unique to CpLCE1 and is reasonably antigenic as determined by various antigenicity indexes using the MacVector v9.5.2 program (MacVector, Inc.). Initially, sera from six pathogen-free rats were collected prior to the immunization protocol, of which preimmune sera from two of the six showed no reactivity to dot blot tests using parasite protein extracts. The synthetic peptide was freshly cross-linked to keyhole limpet hemocyanin prior to each immunization. Polyclonal antibodies to CpLCE1 were raised in two pathogen-free rats that were initially immunized with 200 mg of antigen emulsified in an equal volume of Freund complete adjuvant. Booster immunizations (100 mg) were performed at 30 and 60 days, respectively, after the primary immunization. Rat sera were then collected after the immunization protocol, and specificity of the rat polyclonal antibodies was evaluated by dot and Western blot analyses with protein extracts of parasites and host cells.

Immunofluorescence microscopy. Sporozoites and intracellular developmental stages for immunolocalization analysis were obtained as described above. Intracellular parasites were obtained by infecting human HCT-8 cells grown on glass coverslips treated with poly-L-lysine for 12, 36, or 60 h. Samples were fixed with 10% formalin, rinsed with PBS, and extracted with cold methanol (−20°C). Free sporozoites were applied directly to poly-L-lysine-treated coverslips, air dried, and then extracted. Cells were then blocked with 0.5% bovine serum albumin (BSA)–PBS for 10 min before incubation with primary antibodies for 1 h in 0.5% BSA–PBS. Free sporozoites were then labeled with anti-rat immunoglobulin (IgG) secondary antibodies conjugated with fluorescein isothiocyanate (FITC) for 1 h in 0.5% BSA–TBS. Intracellular developmental stages were all exposed to a 1-h incubation in 0.5% BSA–PBS with anti-rat IgG–tetramethyl rhodamine isocyanate (TRITC) to visualize CpLCE1 localization. Colocalization of CpLCE1 with *C. parvum* fatty acyl-CoA binding protein (CpACBP1) and with total membrane proteins (TMPs) was similarly performed. The anti-TMP antibodies and FITC-conjugated secondary antibodies were incubated simultaneously with anti-CpLCE1 and corresponding secondary antibodies, respectively; whereas the CpACBP1 antibodies were directly labeled with Alexa Fluor 488 using the appropriate fluorophore labeling kit (Invitrogen). Colocalization of CpLCE1 with TMP or CpACBP1 was selected because the TMP antibodies have been shown to label the parasitophorous vacuolar membrane (PVM) and feeder organelle (7) and CpACBP1 localizes to the surface of merozoites as well as colocalizes with TMPs (35). All samples were mounted with a SlowFade Gold antifade reagent containing 4′,6′-diamidino-2-phenylindole (DAPI) for DNA counterstaining (Invitrogen) and examined with an Olympus BX51 epifluorescence microscope equipped with differential interference contrast and TRITC/FITC/DAPI filters.

Cloning and expression of CpLCE1. The 972-bp Cp*LCE1* gene was amplified from *C. parvum* (Iowa strain) genomic DNA using the high-fidelity *Pfu* Ultra DNA polymerase (Stratagene) with the primer sets CpLCE1-Fwd (5′ gcg aat tcA TGT TCA TAG AAA ATA ATA ATA AT 3′) and CpLCE1-Rev (5′ gct cta gaA TCG CGC TTA GTT GGT TTT T 3′) (lowercase represents artificial EcoRI and XbaI linkers, respectively). The amplified product was directly ligated into

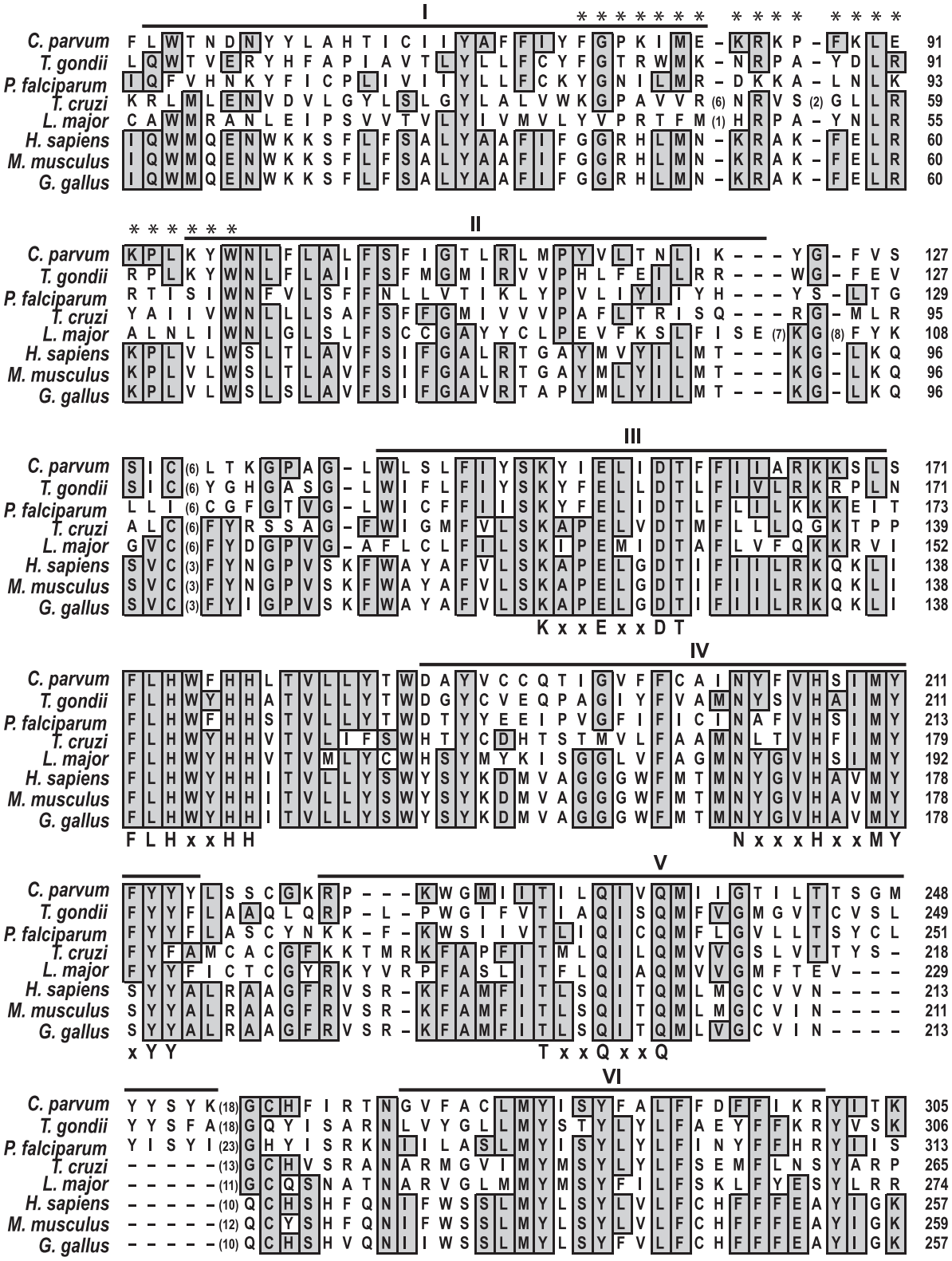

FIG. 2. Amino acid sequence comparison of CpLCE1 and representative eukaryotic elongase condensing enzymes. The cDNA-derived amino acid sequence of CpLCE1 (accession no. AAO34582) is aligned with the deduced sequences of *Toxoplasma gondii* (20.m00392), *Plasmodium falciparum* (XP_001351023), *Trypanosoma cruzi* (XP_813971), *Leishmania major* (CAJ03003), *Homo sapiens* (NP_076995), *Mus musculus* (NP_569717), and *Gallus gallus* (NP_001026710). Amino acids with at least 50% conservation between CpLCE1 and other sequences are shaded. The four highly conserved domains characteristic of the elongase family of enzymes are indicated below the sequence, and the six predicted transmembrane domains are clearly outlined (labeled I to VI). Asterisks indicate the epitope used for antibody production.

the pcDNA3.1/HisC mammalian expression vector (Invitrogen) and transformed into *Escherichia coli* TOP10 cells (Invitrogen).

Plasmid DNA containing the correct insert (pcDNA3.1/HisC-CpLCE1) and confirmed by sequencing was transfected into human embryonic kidney (HEK)-293T cells. HEK-293T cells were plated in 100-mm tissue culture plates and grown at 37°C in an atmosphere of 5% CO_2 in Dulbecco's modified Eagle medium (high glucose) supplemented with 10% fetal bovine serum. At ~90% confluence the pcDNA3.1/HisC-CpLCE1 plasmid or the empty plasmid pcDNA3.1/HisC (10 μg) was transfected into cells using Lipofectamine 2000 (Invitrogen) according to the manufacturer's protocol. After transfection, cells were grown for 48 h at 37°C in Dulbecco's modified Eagle medium plus 10% fetal bovine serum.

Confirmation of transfection and protein expression. At 48 hours after transfection of HEK-293T cells, total RNA was isolated from CpLCE1- and pcDNA3.1/HisC-transfected cultures and nontransfected cultures (as a negative control) using an RNeasy minikit (QIAGEN) following the manufacturer's protocol. The vector-specific T7-Fwd and BGH-Rev primers were used in conjunction with the one-step RT-PCR kit (QIAGEN) to confirm positive transfection.

Transfections were also performed in a 24-well format to assess protein expression using immunofluorescence microscopy. Cells were first seeded onto glass coverslips treated with poly-L-lysine and transfected with CpLCE1 or pcDNA3.1/HisC using the method described above while following the recommended protocol for Lipofectamine 2000 transfection in the 24-well format. After incubation for 48 h, cells were fixed with 10% formalin, rinsed with PBS, extracted with −20°C methanol for 5 min, and blocked in 0.5% BSA–PBS for 10 min. Cells were then labeled with anti-CpLCE1 primary antibodies for 1 h in 0.5% BSA–PBS, followed by incubation with secondary antibodies conjugated with TRITC for 1 h in 0.5% BSA–PBS. The samples were washed after each incubation step three times with PBS for 5 min each. All samples were mounted using DAPI and examined using an Olympus BX51 epifluorescence microscope equipped with differential interference contrast and TRITC/DAPI filters. Cultures that were not transfected or that were transfected with pcDNA3.1/HisC were used as negative controls.

Preparation of total membrane transfected cells. TMP fractions were prepared in a method similar to that for preparing microsomal protein (18). At 48 hours posttransfection, cells were washed with PBS and scraped into 5 ml of ice-cold 250 mM sucrose, 20 mM HEPES (pH 7.5) containing a mammalian protease inhibitor cocktail (Sigma). After centrifugation at 1,000 × *g* for 7 min at 4°C, the cell pellet was resuspended in 3 ml of ice-cold sucrose-HEPES with protease inhibitors. The sample was then Dounce homogenized and centrifuged at 1,000 × *g* at 4°C to remove large cellular debris. The supernatant was then centrifuged at 100,000 × *g* for 1 h at 4°C. The supernatant was discarded, and the resulting pellet was resuspended in 500 μl of 100 mM Tris-HCl, 0.1% Triton X-100 (pH 7.4). Protein concentration was determined by a Bradford colorimetric method using BSA as a standard. Aliquots were snap frozen in liquid nitrogen and stored at −80°C. Western blot analysis using the rat anti-CpLCE1 antibodies and monoclonal rabbit anti-rat IgG antibodies was also performed to test for the presence of CpLCE1 in the prepared membrane fractions of transfected cells.

Fatty acyl-CoA elongation assay. Initial activity of the elongation of fatty acyl-CoA by CpLCE1 was determined using variations of a mixture of previously described methods (18, 22, 30, 32). To optimize reaction conditions, a 100-μl reaction mixture containing 50 mM potassium phosphate (pH 6.5), 5 μM rotenone, 20 μM fatty acid-free BSA, 1 mM $MgCl_2$, 0.5 mM NADH, 0.5 mM NADPH, 60 μM palmitoyl-CoA, and 200 μM [2-^{14}C]malonyl-CoA was heated at 37°C for 2 min. The reaction was started with the addition of 30 μg of protein from CpLCE1- or pcDNA3.1/HisC-transfected cells and allowed to proceed for 30 min at 37°C before the addition of 100 μl of 5N KOH in 10% methanol. The samples were then saponified at 65°C for 1 h and cooled to room temperature, when 100 μl each of 5 N HCl and ethanol were added. Radiolabeled incorporated fatty acids were then extracted from the mixture using 1 ml of hexane followed by vigorous mixing and centrifugation at 10,000 × *g* for 2 min. The upper organic phase was removed, while the lower aqueous phase was washed twice more with 1 ml of hexane. The hexane extracts were pooled and dried under vacuum, and then 5 ml of scintillation fluid was added and the radioactivity was counted in a Beckman Coulter LS 6000SE counter. Activity was determined by subtracting the values obtained for the pcDNA3.1/HisC-transfected samples from the values obtained for the CpLCE1-transfected samples. Reaction mixtures containing no membrane protein were also used as controls to determine additional background levels.

Dependence on NADH or NADPH was determined using the same assay, and the optimum pH for this enzyme was determined using the reaction described above with inclusion of 50 mM potassium phosphate buffer at pH 5.0, 5.5, 6.0, and 6.5 and 50 mM Tris buffer at pH 7.0, 7.5, 8.0, and 8.5. The kinetics for CpLCE1 were similarly assayed using various amounts of palmitoyl-CoA (0.98 to 250 μM), malonyl-CoA (0.98 to 500 μM), and NADPH (3.9 μM to 1 mM).

Substrate preference. Once optimal reaction parameters were known, the substrate preference for CpLCE1 was determined. The fatty acyl-CoA elongation assay used was similar to that described above except it lacked NADH (included 500 μM NADPH) and included 125 μM of various saturated ($C_{2:0}$ to $C_{24:0}$) and unsaturated ($C_{18:1}$, $C_{18:3}$, $C_{20:4}$, and $C_{22:6}$) fatty acyl-CoAs and 250 μM [2-^{14}C]malonyl-CoA. Reaction mixtures included protein fractions from either CpLCE1- or pcDNA3.1/HisC-transfected samples. Activity was determined by subtracting values obtained for the pcDNA3.1/HisC-transfected samples from the values obtained for the CpLCE1-transfected samples. Additionally, substrate preference data were used to test the inhibitory effect of cerulenin, a known inhibitor of both type I and II β-ketoacyl-CoA synthase, on CpLCE1 using the same reaction conditions as described above and including 0.2 to 200 μM cerulenin.

TLC analysis of elongated fatty acids. The fatty acid elongation reaction was assayed as described above using 30 μg protein from either CpLCE1- or pcDNA3.1/HisC-transfected cells, 250 μM nonradiolabeled malonyl-CoA, and 125 μM of either myristoyl-CoA or palmitoyl-CoA ($C_{14:0}$-CoA and $C_{16:0}$-CoA, respectively). Reactions were terminated and fatty acids were extracted as described above. Hexane fractions containing the elongated fatty acids were dried by evaporation under nitrogen before the addition of 3 ml methanol-toluene-sulfuric acid (88:10:2, vol/vol) to convert the extracted fatty acids into their fatty acid methyl ester (FAME) derivatives (11, 30). The suspension was incubated for 1 h at 80°C and allowed to cool to room temperature, and FAMEs were extracted two times with 2 ml hexane. The hexane fractions were once again allowed to evaporate to dryness under nitrogen and were resuspended in 40 μl hexane for thin-layer chromatography (TLC) analysis. Reverse-phase LKC18 silica gel 60-Å TLC plates (Whatman, Inc.) were washed with chloroform-methanol (1:1), followed by incubation at 110°C for 1 h and cooling to room temperature before samples were spotted. The elongated products were separated using methanol-chloroform-water (15:5:1) with authentic FAME standards (Supelco) (25).

HPLC analysis of elongated fatty acids. The elongation assay and FAME preparation used for high-pressure liquid chromatography (HPLC) analysis were replicas of that used for TLC analysis except that the FAMEs were suspended in 200 μl 65% acetonitrile in water instead of 40 μl hexane. FAME derivatives of the elongation products were separated by reverse-phase HPLC using a Shimadzu Prominence HPLC and a Zorbak SB-C18 semipreparative column (5 μm, 9.4 by 250 mm; Agilent Technologies). Injection volumes were 100 μl, and elution was performed using a binary gradient of 95% acetonitrile–5% water at a flow rate of 1.0 ml/min. The absorbance at 205 nm (A_{205}) was monitored using an SPD-M20A diode array detector, and the retention times of the eluted products were compared to those of known FAME standards (Supelco) originally suspended in 65% acetonitrile.

RESULTS

Sequence comparison of elongases related to CpLCE1. In contrast to the case for many other eukaryotic organisms, Cp*LCE1* is the only elongase gene homologue that can be identified from the *C. parvum* genome. This intronless gene encodes 324 amino acids that share several characteristics with related elongase homologues. Figure 2 displays the CpLCE1 amino acid sequence aligned with those of selected mammalian and protozoan elongases. The *Toxoplasma gondii* elongase sequence had the highest similarity with CpLCE1 (45% identical), while the six others were between 31% and 38% identical. The alignment shows that all the sequences share the characteristic FLHxxHH motif that is conserved among elongases and even fatty acid desaturases. Additionally, the KxxE xxDT, NxxxHxxMYxYY, and TxxQxxQ motifs are present, which are also characteristic among elongases and appear to be highly conserved especially among the polyunsaturated fatty acid elongases (19). Structural analysis of CpLCE1 aligned with these related elongases revealed several hydrophobic domains. Analysis with the TMAP algorithm (26) predicts six transmembrane domains which are clearly indicated. This is

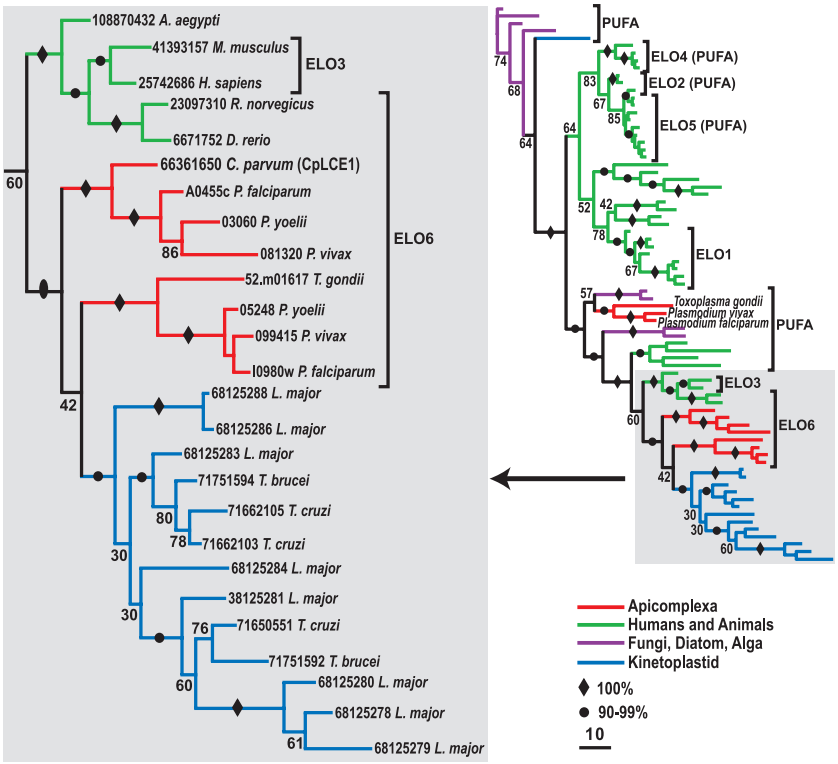

FIG. 3. ML tree derived from 75 elongase sequences (91 amino acid positions) using a Bayesian analysis of phylogeny. PP values at major nodes are indicated as percent values. Solid diamonds, 100%; solid circles, 90 to 99%. These PP values were derived from 3,000 trees obtained after the ML values converged. In the large tree, only the elongase family of proteins are shown as references. The large tree with GenBank gene identification (GI) numbers and species names for all taxa is provided in the supplemental material or can be requested from the corresponding author. Additional ML analysis using the PROML program yielded essentially the same topology shown here.

typical of elongases and confirms the suggestion that CpLCE1 is anchored to a membrane.

Phylogenetic relationships among apicomplexan and other eukaryotic elongases. Thousands of elongase homologues were identified from BLAST searching the GenBank protein databases. Because our goal was to obtain information about the evolution of apicomplexan elongases rather than to take a global approach to analyze the elongase protein family, we constructed phylogenetic trees from a total of 75 taxa from a variety of other organisms. Applying a Bayesian analysis to the phylogeny resulted in distinct groups organized both by the type of elongases and, to a minimal extent, by the taxonomy (Fig. 3). Although the apicomplexan elongases do not form a monophyletic clade, all of the protozoans, including both apicomplexans and the kinetoplastids (*Trypanosoma* and *Leishmania*), remain clustered together. Similar to the case for previous phylogenetic reconstructions (17), the putative kinetoplastid elongases group together in a clade exclusive to this group of parasites. With respect to putative saturated fatty acid elongases among the apicomplexans, they form two clades, both of which appear to be closely related to the ELO6 family of saturated fatty acid elongases.

CpLCE1 is differentially expressed and is localized to the PVM. To determine the CpLCE1 expression pattern in the complex parasite life cycle, real-time qRT-PCR and immunofluorescence detection were performed. Real-time qRT-PCR analysis indicated that the Cp*LCE1* gene is differentially expressed in the *C. parvum* life cycle stages (Fig. 4A). Relative transcript levels also increased at 36 h postinfection (p.i.), and to a minor extent at 60 h p.i., but were detectable at all time points. The free sporozoites (a motile invasive stage of the parasite) exhibited a much higher level of Cp*LCE1* transcripts than all other life cycle stages. The presence of CpLCE1 in protein extracts from sporozoites was clearly displayed by Western blot analysis using polyclonal rat anti-CpLCE1 antibodies (Fig. 4B).

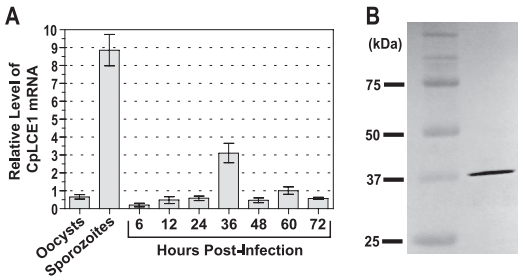

FIG. 4. Expression analysis of the Cp*LCE1* gene in various *C. parvum* life cycle stages. (A) Relative transcript levels were determined using real-time qRT-PCR. The level of transcripts is normalized using the level of *C. parvum* 18S rRNA as a control. For all samples, bars represent the standard errors of the means from triplicate reactions. (B) Western blot analysis using polyclonal rat anti-CpLCE1 antibodies of protein extracted from freshly excysted sporozoites.

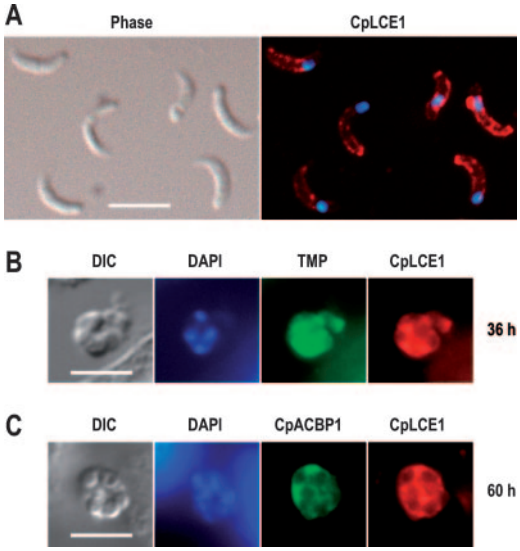

FIG. 5. Immunolocalization of CpLCE1 in free sporozoites and in intracellular life stages. (A) Indirect immunolabeling of freshly excysted sporozoites using rat polyclonal antibodies against CpLCE1 along with secondary antibodies conjugated with TRITC. DAPI, used for counterstaining nuclei, is merged with the image on the right. (B) Colocalization of CpLCE1 (TRITC) with parasite TMPs (FITC) of parasites grown for 36 h. The antibodies against parasite TMPs mainly label the PVM and the electron-dense feeder organelle. (C) Dual labeling of intracellular parasites grown for 60 h indicating that CpLCE1 colocalizes with CpACBP1, which has previously been shown to colocalize with parasite TMPs, most likely at the PVM. Phase, phase-contrast microscopy; DIC, differential interference contrast microscopy. Bars, 5 μm.

Immunofluorescence microscopy indicates that CpCLE1 is present in free sporozoites and localizes to the sporozoite membrane (Fig. 5A). Furthermore, CpLCE1 localizes to the PVM during intracellular development (Fig. 5B and C). This was determined by two separate colocalization studies. Dual-labeling experiments using a rabbit polyclonal antibody mainly against the PVM and the electron-dense feeder organelle colocalized CpLCE1 and PVM proteins (Fig. 5B). It has previously been shown that CpACBP1 also colocalizes with the PVM proteins (35). An additional dual-labeling experiment using rabbit polyclonal antibodies against CpACBP1 colocalized CpLCE1 and CpACBP1 proteins (Fig. 5C). Combined, CpLCE1 localizes to the PVM but not the merozoites within the meronts.

Cloning and expression of CpLCE1. Previous attempts in our laboratory to express and purify recombinant CpLCE1 in bacteria were unsuccessful, typically resulting in the formation of inclusion bodies. However, this is consistent with the elongase family of enzymes, as they tend to have a membrane-bound nature. Therefore, we expressed CpLCE1 in mammalian HEK-293T cells for characterization of this enzyme. HEK-293T cells were used because they offer several advantages. It is widely accepted that this cell line displays a very high level of transfection efficiency. This, in combination with using the pcDNA3.1/HisC expression vector, allows for high-level nonreplicative transient expression. Additionally, these cells also contain their own native elongase system. Thus, recombinant CpLCE1 acts in conjunction with the native HEK-293T elongase system in order to carry out the entire two-carbon fatty acid elongation cycle. However, this can sometimes be a disadvantage due to recombinant and native elongase enzymes competing for the same substrate. This often results in a relatively high degree of background activity that must be taken into consideration when interpreting data obtained from using a heterologous assay system.

Successful transfection and protein expression using this method were analyzed using RT-PCR, Western blotting, and immunolabeling. Total RNA was isolated from cells transfected with either CpLCE1 or pcDNA3.1/HisC (and nontransfected cells as a negative control) at 48 h after transfection, and vector-specific primers were used during RT-PCR to confirm positive transfection. Amplicons of the correct size corresponding to pcDNA3.1/HisC- and CpLCE1-transfected cells were observed (259 bp and 1,195 bp, respectively) (Fig. 6A).

Western blot analysis of the membrane fractions using rat polyclonal antibodies against CpLCE1 clearly confirmed that CpLCE1 is expressed and indicated that it is contained in the purified membrane fractions (Fig. 6B). Immunofluorescence microscopy indicated that this protein was expressed relative to cells transfected with pcDNA3.1/HisC or nontransfected cells (Fig. 6C). The fluorescent signal was largely increased for the CpLCE1-transfected cells and could be observed using a relatively low exposure time (280 ms). At the same exposure there was no observed fluorescent signal from pcDNA3.1/HisC-transfected or nontransfected cells. Only at an exposure time of 9.8 s did a fluorescence signal begin to appear in these samples (Fig. 6C, insets) indicating that the CpLCE1-transfected cells were indeed expressing the desired protein.

Determination of enzyme activity. It is imperative that we first clarify the elongation assay in order for the results to be appropriately understood. The membrane preparations of HEK-293T cells used in this study contain all four enzymes of the elongase system. Thus, in samples that have been transfected with CpLCE1, there are two sets of condensing enzymes which are responsible for the incorporation of ^{14}C from [2-^{14}C]malonyl-CoA. The products formed during the initial condensation reaction (catalyzed by the native elongase and by CpLCE1) then proceed through the subsequent three steps of the elongation system (β-ketoacyl-CoA reductase, β-hydroxyacyl-CoA dehydratase, and enoyl-CoA reductase) to produce a final two-carbon extended product (see Fig. 1 for reaction details). Therefore, there is detectable background activity that is present when using this heterologous system and must be distinguished from activity produced by recombinant CpLCE1.

Total fatty acid elongation activity was measured in isolated membrane fractions of HEK-293T cells transfected with CpLCE1 and compared with that in HEK-293T cells transfected with the empty vector alone (pcDNA3.1/HisC). Supernatant fractions resulting from the membrane purification process were also used as controls. Palmitoyl-CoA ($C_{16:0}$-CoA) was initially chosen as the fatty acid substrate for the elongation assay, which measured the incorporation of ^{14}C from [2-^{14}C]malonyl-CoA into elongated fatty acid products. Total elongation activity was increased in the membrane fractions from CpLCE1-transfected cells compared to cells transfected with the empty vector (Fig. 7A). The activities detected in the supernatant fractions of CpLCE1- and pcDNA3.1/HisC-transfected cells were not significantly different from each other but

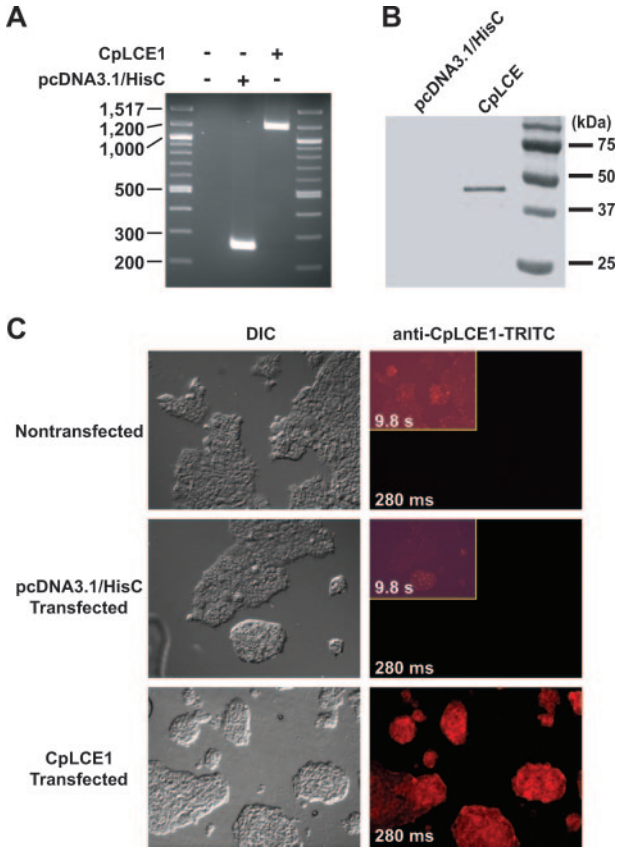

FIG. 6. Confirmation of successful transfection and expression of CpLCE1. (A) At 48 h posttransfection, total RNA was isolated from cells transfected with CpLCE1 or the empty vector and from nontransfected cells. RT-PCR analysis viewed on a 2% agarose gel indicated that both the vector and the vector containing the CpLCE1 construct were effectively transfected. (B) Western blot analysis of the purified membrane fractions from cells transfected with CpLCE1 or pcDNA3.1/HisC. Eighty micrograms of protein from each fraction was separated on a 10% sodium dodecyl sulfate-polyacrylamide gel, transferred to nitrocellulose, and labeled with rat polyclonal antibodies against CpLCE1. Further incubation with rabbit anti-rat antibodies conjugated to alkaline phosphatase followed by development with 5-bromo-4-chloro-3-indolylphosphate resulted in a single band corresponding to CpLCE1. (C) Immunofluorescence detection of CpLCE1 protein expression. Nontransfected cells were used as a negative control. Clearly, the fluorescence intensity when labeling with rat anti-CpLCE1 antibodies followed by rabbit anti-rat IgG conjugated to TRITC was highest in cells transfected with CpLCE1. A 35-fold increase in exposure time (280 ms versus 9.8 s) was required to detect only minor fluorescence intensity in pcDNA3.1/HisC-transfected cells (comparable to nontransfected cells; both are shown as insets).

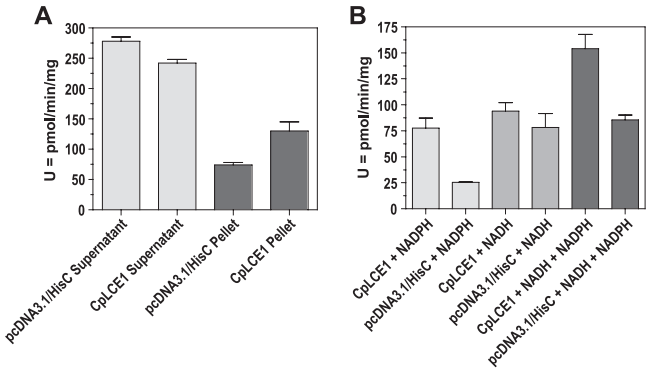

FIG. 7. Elongase activity determination and NADPH dependence. (A) The final pellet fraction after membrane purification of CpLCE1-transfected cells displayed higher elongase activity than that from cells transfected with the empty vector. Both NADH and NADPH were used as cosubstrates. The high activity observed in the soluble fractions likely results from soluble proteins utilizing malonyl-CoA and NAD(P)H. (B) Total elongation activity as measured when including various combinations of NAD(P)H. As expected, the most significant difference among fractions containing CpLCE1 and control fractions was observed when using NADPH as the sole cosubstrate. Values were obtained by subtracting the activity detected using fractions from cells transfected with the empty vector. Values are represented as pmol/min/mg of TMP. In all samples, bars represent the standard errors of the means from triplicate reactions.

were significantly higher than the activity detected in the membrane fractions (Fig. 7A). The activity in the supernatant fractions is expected due to the soluble enzymes that use malonyl-CoA as a cosubstrate, such as the soluble FAS enzymes. Thus, in agreement with Western blot and immunofluorescent analysis (Fig. 6B and C, respectively) the CpLCE1 activity is contained in the membrane fractions of cells transfected with CpLCE1.

To further confirm that the observed activity was indeed that of the elongase complex, we separately incubated membrane fractions with or without NAD(P)H (Fig. 7B). When NADH was used as a cosubstrate, activity was detected in both the CpLCE1- and pcDNA3.1/HisC-transfected samples; however, these activities were not significantly different from each other, confirming that the subsequent reduction reactions of the elongation system do not utilize NADH as a cosubstrate. The activity observed here is due to a partial contribution of other membrane enzymes that make use of NADH. When NADPH was used as the sole cosubstrate, the membrane fractions from the CpLCE1-transfected cells displayed a significantly greater elongation activity than those from the cells transfected with the vector alone. Combined, these data confirm that NADPH is the required cosubstrate for the elongation system reduction reactions and that CpLCE1 is capable of carrying out the initial reaction of the elongase system.

Optimization of CpLCE1 assay and enzyme kinetics. Because palmitoyl-CoA could serve as a substrate for CpLCE1, it was used to optimize the conditions of the elongation reaction prior to testing additional fatty acid substrates to determine substrate specificity. The highest rate of [^{14}C]malonyl-CoA incorporation into elongated fatty acid products was observed when the concentration of palmitoyl-CoA was 125 μM (Fig. 8A). Additionally, enzyme kinetics analysis revealed that CpLCE1 displayed typical Michaelis-Menten kinetics towards palmitoyl-CoA ($h = 1$, $K_m = 73.30$ μM, and $V_{max} = 67.64$ U [1 U = 1 pmol/min/mg of TMP]) (Fig. 8A). However, further analysis indicated that the CpLCE1 kinetics actually fit better to a sigmoidal curve ($r^2 = 0.9707$ versus 0.9577), indicating the presence of positive cooperativity (Fig. 8A). Under the consideration of cooperativity, the values for K_{50} (equivalent to K_m) and V_{max} were determined to be 43.76 μM and 52.74 U, respectively. Analysis of the kinetics of CpLCE1 towards malonyl-CoA revealed similarities to that observed towards palmitoyl-CoA. While the optimal concentration of malonyl-

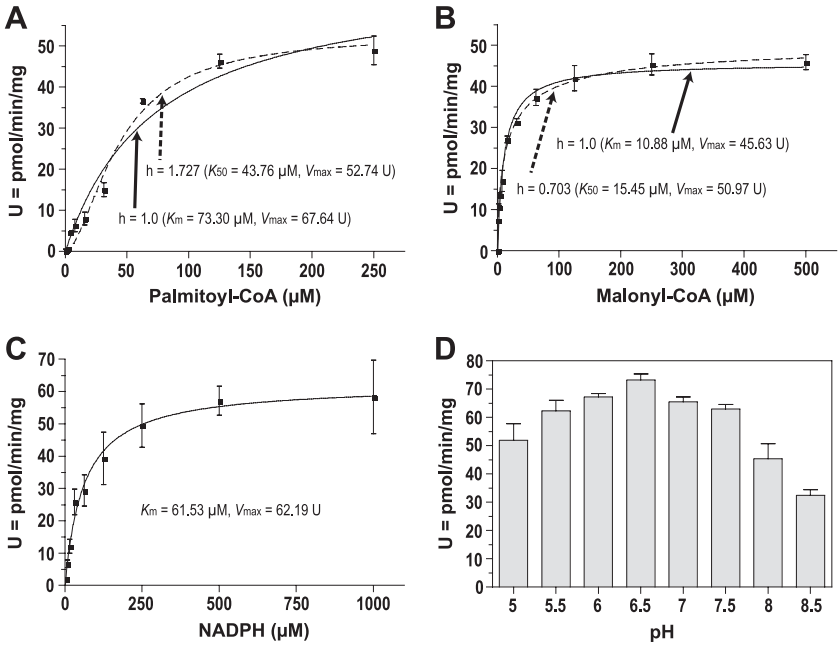

FIG. 8. Enzyme kinetics of the condensation reaction and kinetics and pH optimum for the overall elongation system. (A) Allosteric kinetics assayed with various concentrations of palmitoyl-CoA indicates the presence of positive cooperativity in the condensation reaction (Hill coefficient [h] = 1.727). The optimum palmitoyl-CoA concentration was 125 μM. (B) Allosteric kinetics assayed with various concentrations of malonyl-CoA indicates the presence of negative cooperativity (h = 0.703) with an optimum concentration of 250 μM. (C) Enzyme kinetics assayed with various concentrations of NADPH. As the two reduction steps of the elongation system require NADPH, the results show that when using palmitoyl-CoA as a substrate and CpLCE1 as the condensing enzyme, the elongase system displays general Michaelis-Menten kinetics. (D) The optimum pH of the condensing enzyme is 6.5. Values were obtained by subtracting the activity detected using fractions from cells transfected with the empty vector. Values are represented as pmol/min/mg of TMPs. For all samples, bars represent the standard errors of the means from triplicate reactions.

CoA was 250 μM, CpLCE1 displayed a slightly better fit to a sigmoidal curve (Fig. 8B) (r^2 = 0.9387). This is a slight negative cooperativity with a K_{50} of 15.45 μM and a V_{max} of 50.97 U compared to the general Michaelis-Menten kinetics (Fig. 8B) (r^2 = 0.9265). When using increasing concentrations of NADPH, general Michaelis-Menten kinetics were observed (Fig. 8C), with a K_m of 61.53 μM and a V_{max} of 62.19 U, and the optimum concentration of NADPH was 500 μM. The observed NADPH kinetics are in respect to the two reduction reactions that occur as a result of activity initiated by CpLCE1, the condensation reaction. Fatty acid elongation activity was also determined to be highest at a pH optimum of 6.5 (Fig. 8D).

CpLCE1 displays the highest activity towards $C_{14:0}$ and $C_{16:0}$. Using the optimal assay conditions found above, we determined the substrate specificity of CpLCE1 using a wide range of fatty acyl-CoAs. Figure 9 shows the total fatty acid elongation activity in membrane fractions from CpLCE1-transfected HEK-293T cells using even-carbon saturated fatty acyl-CoAs from $C_{2:0}$ to $C_{24:0}$ and the unsaturated (or polyunsaturated) fatty acyl-CoAs $C_{18:1}$, $C_{18:3}$, $C_{20:4}$, and $C_{22:6}$. Compared to membrane fractions from pcDNA3.1/HisC-transfected cells, the cells expressing recombinant CpLCE1 displayed significantly higher elongase activities when assayed with the medium- to long-chain fatty acyl-CoAs $C_{10:0}$ to $C_{18:0}$ and the highest with $C_{14:0}$ and $C_{16:0}$. Relatively little to no activity above background was detected when short- or very-long-chain fatty acyl-CoAs were used as substrates. Interestingly, arachidonic acid ($C_{20:4}$) was the only unsaturated fatty acid that displayed a rather significant activity above background. This was not expected and is considered to be an artifact due to in vitro assay conditions.

Analysis of elongation products. The two fatty acyl-CoAs shown to display the highest elongated activity when used as substrates (myristoyl-CoA and palmitoyl-CoA) were used to analyze the elongated products by both TLC and HPLC. Upon completion of the reaction, the elongation fatty acid products were methylated to their methyl ester derivatives for comparison with FAME standards. When elongation products of membrane fractions from CpLCE1-transfected cells were analyzed using reverse-phase TLC, the major products were palmitic acid ($C_{16:0}$) and stearic acid ($C_{18:0}$) when incubated

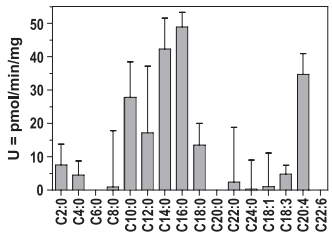

FIG. 9. Substrate specificity of CpLCE1. Saturated fatty acyl-CoAs from $C_{2:0}$ to $C_{24:0}$ and various unsaturated fatty acyl-CoAs were used to determine the substrate preference of the condensing enzyme. Values were obtained by subtracting the activity detected using fractions from cells transfected with the empty vector. Values are represented as pmol/min/mg of TMPs. For all samples, bars represent the range of values from two sets of triplicate reactions.

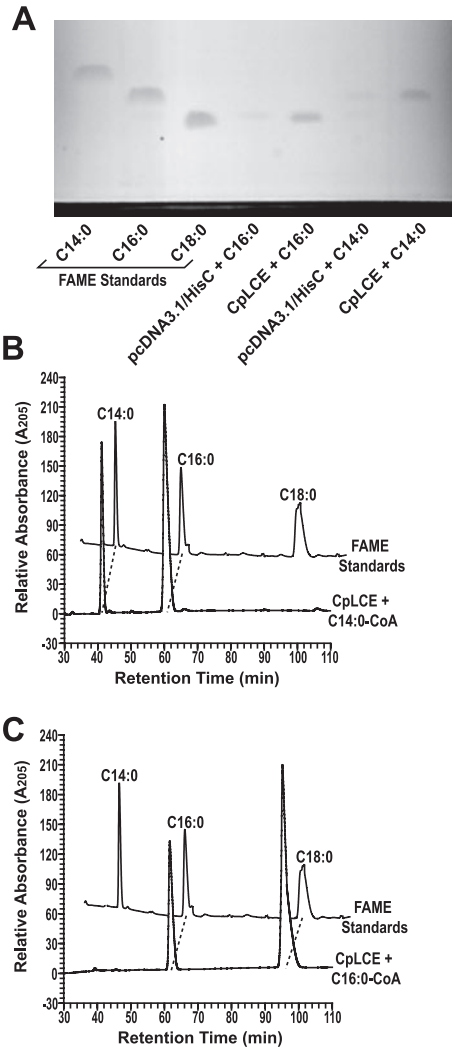

FIG. 10. Fatty acid elongation product analysis using TLC and HPLC. (A) The products of fatty acid elongation were converted to their methyl ester derivatives for analysis using reverse-phase TLC. Both myristoyl-CoA and palmitoyl-CoA ($C_{14:0}$ and $C_{16:0}$, respectively) were used as substrates based on the substrate preference data. (B) HPLC analysis of elongation products converted to methyl esters is comparable to that using TLC. The data show that only one round of elongation occurs regardless of the fatty acyl substrate used. Retention times of all samples were compared to those of authentic fatty acid methyl standards. HPLC peaks were detected as A_{205}.

with myristoyl-CoA ($C_{14:0}$) or palmitoyl-CoA ($C_{16:0}$), respectively (Fig. 10A). As a background control, membrane fractions from cells transfected with pcDNA3.1/HisC were also analyzed using TLC. The major product of the control when using palmitoyl-CoA as a substrate was stearic acid. However, when incubated with myristoyl-CoA, there were two products detected on TLC, palmitic acid and stearic acid, indicating that membrane fractions not transfected with CpLCE1 were capable of additional rounds of elongation. In either case, the production of a two-carbon elongated product by the CpLCE1-transfected cells resulted in a significantly larger quantity than that with the pcDNA3.1/HisC-transfected samples.

To ensure that only one round of elongation was occurring

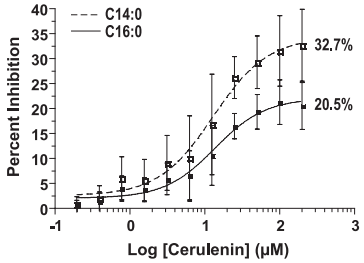

FIG. 11. Inhibitory effect of cerulenin on the activity of CpLCE1. The inhibition effects when using both myristoyl-CoA ($C_{14:0}$) and palmitoyl-CoA ($C_{16:0}$) were assayed. Values were obtained by subtracting the activity detected using fractions from cells transfected with the empty vector. Values are represented as total [^{14}C]malonyl-CoA incorporation (pmol) based on a total of 30 μg membrane protein. For all samples, bars represent the range of values from two sets of triplicate reactions.

in membrane fractions transfected with CpLCE1, the elongation products were also analyzed using HPLC. If additional rounds of elongation were indeed occurring, then the higher-sensitivity HPLC analysis would detect multiple products. Similar to analysis of the elongation reaction with TLC, FAMEs were derived from the elongated products for comparison to methyl ester standards. Analysis by HPLC agreed with TLC analysis, further indicating that only one round of elongation occurs in the CpLCE1-transfected samples. When incubation was with myristoyl-CoA as a substrate, palmitic acid was detected (Fig. 10B), and when palmitoyl-CoA was used as a substrate, the addition of two carbons resulting in stearic acid was detected (Fig. 10C). In both instances, the substrate was also detected, indicating that not all substrate was converted into an elongated product.

Inhibition of elongation by cerulenin. Cerulenin is a common eukaryotic and bacterial β-ketoacyl-[acyl carrier protein] synthase inhibitor. Initially, we tested its inhibitory effects using palmitoyl-CoA as the substrate, where cerulenin displayed a maximum inhibition of 20.5% at a concentration of 200 μM (Fig. 11, solid line). Because differential inhibition of cerulenin has been shown to occur depending on fatty acid chain length (23), we also tested inhibition with myristoyl-CoA as a substrate. However, similar to the case with palmitoyl-CoA as a substrate, cerulenin displayed a maximum inhibition of 32.7% at a concentration of 200 μM (Fig. 11, dotted line). Thus, CpLCE1 appears to be relatively insensitive to cerulenin up to 200 μM when both myristoyl-CoA and palmitoyl-CoA are used as substrates.

DISCUSSION

Among the apicomplexans, CpLCE1 is the first elongase to be studied, and it is one of very few studied among the parasitic protists. It is interesting that the *C. parvum* genome encodes only one elongase, whereas both *T. gondii* and *Plasmodium falciparum* contain three. However, differences in fatty acid metabolism (and lipid metabolism in general) among these organisms do exist. Among the apicomplexans that possess a plastid and associated type II FAS, *P. falciparum* lacks a type I FAS or polyketide synthase (PKS), but *T. gondii* and *Eimeria tenella* both possess a type I FAS and PKS (40). Similarly, *C.*

parvum contains only a type I FAS and PKS (10, 38, 39, 41). Thus, it is not a surprise that *C. parvum*, with its very streamlined metabolism, contains only one elongase.

Generally, fatty acid elongases are divided into two groups: (i) those involved or suspected to be involved in the elongation of saturated and monounsaturated fatty acids and (ii) those that are responsible for elongation of polyunsaturated fatty acids (13). Those of the first group are typically of the ELO1, -3, and -6 families, whereas the latter group consists of the ELO2, -4, and -5 families. Molecular analyses of CpLCE1 indicated that it contains structural characteristics possessed by the elongase family, including four highly conserved motifs and several predicted transmembrane domains. Furthermore, phylogenetic reconstructions indicate that CpLCE1 is contained within the ELO6 family. This family is suggested to be involved in the elongation of $C_{12:0}$ to $C_{16:0}$ saturated fatty acid substrates to $C_{18:0}$ products and do not have the ability to elongate beyond $C_{18:0}$ (13). The majority of the kinetoplastid elongases analyzed form a clade with the ELO6-like apicomplexan elongases, suggesting that all of these originated from a common ancestor. Additionally, CpLCE1 appears to be more distant from unsaturated elongase families.

Real-time qRT-PCR indicated that Cp*LCE1* transcript levels are expressed in all stages of the *C. parvum* life cycle but are highest in the sporozoites, followed by stages at 36 h and 60 h p.i. In addition to membrane localization in sporozoites, immunostaining has localized CpLCE1 primarily to the PVM, similar to the case for both CpACBP1 and the *C. parvum* oxysterol binding protein-related protein 1 (CpORP1) (35, 36). *Cryptosporidium parvum* is an intracellular parasite, but it is considered extracytoplasmic because of being covered by a PVM on the host intestinal epithelial cells (6). Although association with the feeder organelle is still undetermined, it is interesting that CpLCE1 localizes to the PVM along with CpACBP1 and CpORP1, which could possibly be involved in lipid uptake across the PVM (35, 36). Whether CpLCE1 acts in conjunction with these two in either lipid uptake or formation of the PVM is not understood at this time. Regardless, PVM proteins may serve as prime chemotherapeutic and/or immunotherapeutic targets in this parasite, for which fully effective treatment is currently unavailable.

The extreme hydrophobicity of elongase proteins has caused many difficulties in the solubilization and purification of these membrane-bound condensing enzymes and has greatly hindered the biochemical characterization of their defined roles in fatty acid elongation. Nearly all enzymatic studies of these elongase enzymes have been carried out using membrane fractions. Thus, we expressed CpLCE1 in mammalian HEK-293T cells in order to characterize the biochemical features of this enzyme.

Substrate preference revealed that CpLCE1 displays the highest activity when myristoyl-CoA and palmitoyl-CoA ($C_{14:0}$ and $C_{16:0}$, respectively) are used as substrates. This is in agreement with phylogenetic reconstructions that grouped CpLCE1 with the ELO6 family of elongases, which generally prefer $C_{12:0}$ to $C_{16:0}$ as substrates. It is interesting that CpLCE1 showed little to no preference for all other saturated and unsaturated substrates except for arachidonyl-CoA ($C_{20:4}$). It is unknown whether this is due to in vitro effects or whether CpLCE1 would potentially have the ability to elongate $C_{20:4}$ in vivo. Although total lipid analysis studies of *C. parvum* are lacking, one report suggests that $C_{20:4}$ comprises only 0.7% of the total neutral fatty acid content in *C. parvum* and 2.3% and 1.2% in the total phospholipid and phosphatidylcholine content, respectively (20), indicating that $C_{20:4}$ is present in only small amounts in *C. parvum.* However, the C_{22} product of elongation was not detected. No other enzyme involved in *C. parvum* fatty acid metabolism has displayed preference for an unsaturated substrate, which leads us to believe that elongation of arachidonyl-CoA is an assay artifact.

Analyses of the CpLCE1-catalyzed elongation products indicate that only one round of elongation occurs, thus extending the length of each substrate by only two carbons. The factors that determine exactly how many rounds of elongation occur are unknown and could rely on the needs of the individual cell or organism at the time in which elongation occurs. Our substrate preference data indicated that both myristoyl-CoA and palmitoyl-CoA are capable of serving as substrates. However, it is intriguing that the longest-chain product observed when using $C_{14:0}$ as a substrate was $C_{16:0}$. It is not clear why the elongated $C_{16:0}$ does not serve as a substrate itself and undergo another round of elongation. This could be an artifact due to heterologous assay conditions; however, other elongase enzymes expressed and assayed using similar methods clearly demonstrate as many as three rounds of elongation (21).

Cerulenin was shown to have a minimal effect on inhibition of CpLCE1, with a maximal inhibition of 20.5% and 32.7% when using the substrates $C_{16:0}$-CoA and $C_{14:0}$-CoA, respectively. This is interesting due to the ability of cerulenin to efficiently inhibit both type I and type II β-ketoacyl-CoA synthases, which was the case for the control fractions transfected with pcDNA3.1/HisC. At low concentrations of cerulenin (~2.1 μM), activity was inhibited by 80% and remained constant over the tested concentrations (data not shown). The observed activity of cerulenin on CpLCE1 could be due to two factors: (i) the alkyl chain of cerulenin could be too long to bind to the active site of the enzyme (15), or (ii) the active site serving as the target of cerulenin could be somewhat inaccessible due to the extreme hydrophobicity of the enzyme (34). Elongase enzymes of other types and different families from various organisms have also shown differential inhibition by cerulenin. For example, the plant-type elongases appear to be fairly resistant (9, 25), whereas ELO2 and ELO3 but not ELO1 from *Trypanosoma* is susceptible (15). Further analyses on the ELO6 family of enzymes as well as elongase enzymes purified to homogeneity are needed in order to fully and accurately determine the effects of cerulenin.

ACKNOWLEDGMENT

This research was supported by a grant (R01 AI44594) from the National Institutes of Health (NIH) under the U.S. Department of Health and Human Services (DHHS).

REFERENCES

1. **Abrahamsen, M. S., and A. A. Schroeder.** 1999. Characterization of intracellular *Cryptosporidium parvum* gene expression. Mol. Biochem. Parasitol. **104:**141–146.
2. **Altschul, S. F., T. L. Madden, A. A. Schaffer, J. Zhang, Z. Zhang, W. Miller, and D. J. Lipman.** 1997. Gapped BLAST and PSI-BLAST: a new generation of protein database search programs. Nucleic Acids Res. **25:**3389–3402.
3. **Arrowood, M. J., and C. R. Sterling.** 1987. Isolation of *Cryptosporidium* oocysts and sporozoites using discontinuous sucrose and isopycnic Percoll gradients. J. Parasitol. **73:**314–319.

4. **Bernert, J. T., Jr., and H. Sprecher.** 1977. An analysis of partial reactions in the overall chain elongation of saturated and unsaturated fatty acids by rat liver microsomes. J. Biol. Chem. **252:**6736–6744.
5. **Cai, X., D. Herschap, and G. Zhu.** 2005. Functional characterization of an evolutionarily distinct phosphopantetheinyl transferase in the apicomplexan *Cryptosporidium parvum*. Eukaryot. Cell **4:**1211–1220.
6. **Chen, X. M., J. S. Keithly, C. V. Paya, and N. F. LaRusso.** 2002. Cryptosporidiosis. N. Engl. J. Med. **346:**1723–1731.
7. **Chen, X. M., B. Q. Huang, P. L. Splinter, H. Cao, G. Zhu, M. A. McNiven, and N. F. LaRusso.** 2003. *Cryptosporidium parvum* invasion of biliary epithelia requires host cell tyrosine phosphorylation of cortactin via c-Src. Gastroenterology **125:**216–228.
8. **Cinti, D. L., L. Cook, M. N. Nagi, and S. K. Suneja.** 1992. The fatty acid chain elongation system of mammalian endoplasmic reticulum. Prog. Lipid Res. **31:**1–51.
9. **Fehling, E., R. Lessire, C. Cassagne, and K. D. Mukherjee.** 1992. Solubilization and partial purification of constituents of acyl-CoA elongase from Lunaria annua. Biochim. Biophys. Acta **1126:**88–94.
10. **Fritzler, J. M., and G. Zhu.** 2007. Functional characterization of the acyl-[acyl carrier protein] ligase in the *Cryptosporidium parvum* giant polyketide synthase. Int. J. Parasitol. **37:**307–316.
11. **Ghanevati, M., and J. G. Jaworski.** 2001. Active-site residues of a plant membrane-bound fatty acid elongase beta-ketoacyl-CoA synthase, FAE1 KCS. Biochim. Biophys. Acta **1530:**77–85.
12. **Huelsenbeck, J. P., and F. Ronquist.** 2001. MRBAYES: Bayesian inference of phylogenetic trees. Bioinformatics **17:**754–755.
13. **Jakobsson, A., R. Westerberg, and A. Jacobsson.** 2006. Fatty acid elongases in mammals: their regulation and roles in metabolism. Prog. Lipid Res. **45:**237–249.
14. **Jones, D. T., W. R. Taylor, and J. M. Thornton.** 1992. The rapid generation of mutation data matrices from protein sequences. Comput. Appl. Biosci. **8:**275–282.
15. **Lee, S. H., J. L. Stephens, and P. T. Englund.** 2007. A fatty-acid synthesis mechanism specialized for parasitism. Nat. Rev. Microbiol. **5:**287–297.
16. **Leonard, A. E., S. L. Pereira, H. Sprecher, and Y. S. Huang.** 2004. Elongation of long-chain fatty acids. Prog. Lipid Res. **43:**36–54.
17. **Livore, V. I., K. E. Tripodi, and A. D. Uttaro.** 2007. Elongation of polyunsaturated fatty acids in trypanosomatids. FEBS J. **274:**264–274.
18. **Matsuzaka, T., H. Shimano, N. Yahagi, T. Yoshikawa, M. Amemiya-Kudo, A. H. Hasty, H. Okazaki, Y. Tamura, Y. Iizuka, K. Ohashi, J. Osuga, A. Takahashi, S. Yato, H. Sone, S. Ishibashi, and N. Yamada.** 2002. Cloning and characterization of a mammalian fatty acyl-CoA elongase as a lipogenic enzyme regulated by SREBPs. J. Lipid Res. **43:**911–920.
19. **Meyer, A., H. Kirsch, F. Domergue, A. Abbadi, P. Sperling, J. Bauer, P. Cirpus, T. K. Zank, H. Moreau, T. J. Roscoe, U. Zahringer, and E. Heinz.** 2004. Novel fatty acid elongases and their use for the reconstitution of docosahexaenoic acid biosynthesis. J. Lipid Res. **45:**1899–1909.
20. **Mitschler, R. R., R. Welti, and S. J. Upton.** 1994. A comparative study of lipid compositions of *Cryptosporidium parvum* (Apicomplexa) and Madin-Darby bovine kidney cells. J. Eukaryot. Microbiol. **41:**8–12.
21. **Moon, Y. A., N. A. Shah, S. Mohapatra, J. A. Warrington, and J. D. Horton.** 2001. Identification of a mammalian long chain fatty acyl elongase regulated by sterol regulatory element-binding proteins. J. Biol. Chem. **276:**45358–45366.
22. **Moon, Y. A., and J. D. Horton.** 2003. Identification of two mammalian reductases involved in the two-carbon fatty acyl elongation cascade. J. Biol. Chem. **278:**7335–7343.
23. **Morita, Y. S., K. S. Paul, and P. T. Englund.** 2000. Specialized fatty acid synthesis in African trypanosomes: myristate for GPI anchors. Science **288:**140–143.
24. **Nugteren, D. H.** 1965. The enzymic chain elongation of fatty acids by rat-liver microsomes. Biochim. Biophys. Acta **106:**280–290.
25. **Paul, S., K. Gable, F. Beaudoin, E. Cahoon, J. Jaworski, J. A. Napier, and T. M. Dunn.** 2006. Members of the *Arabidopsis* FAE1-like 3-ketoacyl-CoA synthase gene family substitute for the Elop proteins of *Saccharomyces cerevisiae*. J. Biol. Chem. **281:**9018–9029.
26. **Persson, B., and P. Argos.** 1994. Prediction of transmembrane segments in proteins utilising multiple sequence alignments. J. Mol. Biol. **237:**182–192.
27. **Prasitchoke, P., Y. Kaneko, T. Bamba, E. Fukusaki, A. Kobayashi, and S. Harashima.** 2007. Identification and characterization of a very long-chain fatty acid elongase gene in the methylotrophic yeast, Hansenula polymorpha. Gene **391:**16–25.
28. **Rider, S. D., Jr., X. Cai, W. J. Sullivan, Jr., A. T. Smith, J. Radke, M. White, and G. Zhu.** 2005. The protozoan parasite *Cryptosporidium parvum* possesses two functionally and evolutionarily divergent replication protein A large subunits. J. Biol. Chem. **280:**31460–31469.
29. **Robertson, L. J., A. T. Campbell, and H. V. Smith.** 1993. In vitro excystation of *Cryptosporidium parvum*. Parasitology **106:**13–19.
30. **Salas, J. J., E. Martinez-Force, and R. Garces.** 2005. Very long chain fatty acid synthesis in sunflower kernels. J. Agric. Food Chem. **53:**2710–2716.
31. **Smith, S.** 1994. The animal fatty acid synthase: one gene, one polypeptide, seven enzymes. FASEB J. **8:**1248–1259.
32. **Wang, Y., D. Botolin, B. Christian, J. Busik, J. Xu, and D. B. Jump.** 2005. Tissue-specific, nutritional, and developmental regulation of rat fatty acid elongases. J. Lipid Res. **46:**706–715.
33. **White, S. W., J. Zheng, Y. M. Zhang, and Rock.** 2005. The structural biology of type II fatty acid biosynthesis. Annu. Rev. Biochem. **74:**791–831.
34. **Zank, T. K., U. Zahringer, C. Beckmann, G. Pohnert, W. Boland, H. Holtorf, R. Reski, J. Lerchl, and E. Heinz.** 2002. Cloning and functional characterisation of an enzyme involved in the elongation of Delta6-polyunsaturated fatty acids from the moss *Physcomitrella patens*. Plant J. **31:**255–268.
35. **Zeng, B., X. Cai, and G. Zhu.** 2006. Functional characterization of a fatty acyl-CoA-binding protein (ACBP) from the apicomplexan *Cryptosporidium parvum*. Microbiology **152:**2355–2363.
36. **Zeng, B., and G. Zhu.** 2006. Two distinct oxysterol binding protein-related proteins in the parasitic protist *Cryptosporidium parvum* (Apicomplexa). Biochem. Biophys. Res. Commun. **346:**591–599.
37. Reference deleted.
38. **Zhu, G., M. J. Marchewka, K. M. Woods, S. J. Upton, and J. S. Keithly.** 2000. Molecular analysis of a Type I fatty acid synthase in *Cryptosporidium parvum*. Mol. Biochem. Parasitol. **105:**253–260.
39. **Zhu, G., M. J. LaGier, F. Stejskal, J. J. Millership, X. Cai, and J. S. Keithly.** 2002. *Cryptosporidium parvum*: the first protist known to encode a putative polyketide synthase. Gene **298:**79–89.
40. **Zhu, G.** 2004. Current progress in the fatty acid metabolism in *Cryptosporidium parvum*. J. Eukaryot. Microbiol. **51:**381–388.
41. **Zhu, G., Y. Li, X. Cai, J. J. Millership, M. J. Marchewka, and J. S. Keithly.** 2004. Expression and functional characterization of a giant type I fatty acid synthase (CpFAS1) gene from *Cryptosporidium parvum*. Mol. Biochem. Parasitol. **134:**127–135.